Inverse Analyses of Transport of Chlorinated Hydrocarbons Subject to Sequential Transformation Reactions

Francis X. M. Casey* and Jiří Šimůnek

ABSTRACT

Chemical and biological transformations can significantly affect contaminant transport in the subsurface. To better understand such transformation reactions, an equilibrium–nonequilibrium sorption transport model, HYDRUS-1D, was modified by including inverse solutions for multiple breakthrough curves resulting from the transport of solutes undergoing sequential transformations. The inverse solutions were applied to miscible-displacement experiments involving dissolved concentrations of trichloroethylene (TCE) undergoing reduction and/or transformations in the presence of zero-valent metal porous media (i.e., iron or copper-coated iron filings) to produce ethylene. The inverse model solutions provided a reasonable description of the transport and transformation processes. Simultaneous fitting of multiple breakthrough curves of TCE and ethylene placed additional constraints on the inverse solution and improved the reliability of parameter estimates. Confidence intervals of optimized parameters were reduced significantly in comparison with those obtained by fitting TCE breakthrough curves independently. Further evidence for accurate parameter estimates was given when the parameter values agreed with previously reported values from independent batch and degradation experiments. Optimized values of the normalized degradation rates for the equilibrium (1.4×10^{-4} to 7.2×10^{-5} L h^{-1} m^{-2}) and nonequilibrium (1.2×10^{-4} to 5.5×10^{-5} L h^{-1} m^{-2}) models compared well with values (0.03 to 6.5×10^{-5} L h^{-1} m^{-2}) obtained from previous studies. The estimated TCE–iron sorption coefficients (0.52 to 2.85 L kg^{-1}) were also consistent with a previously reported value (1.47 L kg^{-1}).

Transformation processes, such as biotransformation and radioactive decay, are very common and have major influence on the movement of contaminants in porous media. Examples of solutes undergoing various transformation reactions and migration in the soil include radionuclides (Evans et al., 1997; Viswanathan et al., 1998), nitrogen species (Mishra and Misra, 1991; Misra et al., 1974), organic phosphates (Castro and Rolston, 1977), and organic hydrocarbons (Burt, 1999; Schaerlaekens et al., 1999). These reactions are frequently identified and modeled as linear, instantaneous processes; however, they can often be much more complex. Solutes involved in transformation reactions in addition to nonideal transport greatly confound the study, modeling, and prediction of solute transport. There is a need for modeling techniques that can help identify these processes by unraveling the complexity.

Several models exist, such as CHAIN (van Genuchten et al., 1985), which can describe the transport of solutes undergoing ideal first-order transformation reactions. CHAIN, an analytical equilibrium, one-dimensional convection–dispersion transport model, has been expanded to include nonequilibrium transport and transient water flow within the numerical model, HYDRUS-1D (Šimůnek et al., 1998a). Inverse methods (van Genuchten, 1981; Kool et al., 1985) have become the standard in soil science to identify solute transport parameters, and have been shown to be very successful. Nonetheless, there still has been little inverse application of transport models to solutes that undergo transformation and to their degradation daughter products. Inverse application of these transformation transport models can lead to better identification of transport processes, which can increase our understanding and lead to better prediction.

Ground water contamination by chlorinated aliphatic hydrocarbons (CAHs) is an area that reflects the importance of having methods that can lead to deeper understanding of solutes undergoing transport and transformation. The prevalent use of CAHs as industrial solvents and in dry cleaning operations has caused widespread ground water contamination. The National Academy of Sciences identified TCE, a CAH, as the most common contaminant at nearly 300 000 to 400 000 hazardous waste sites in the USA (National Academy of Science, 1994). Ground water remediation of CAHs by zero-valent metals shows promise because of its relatively low costs and the virtual elimination of the CAHs and their degradation daughter products (Focht et al., 1996; Appleton, 1996). It is theorized that CAHs in the presence of zero-valent metals, such as iron filings, undergo a reduction process where electrons are exchanged between the pollutant molecule and an electron donor (i.e., zero-valent metal). In the reduction of TCE (C_2HCl_3), there is sequential removal of chloride ions, which produces dichloroethylene isomers ($C_2H_2Cl_2$) that are further reduced to vinyl chloride (C_2H_3Cl), then ethylene (C_2H_4), and finally ethane (C_2H_6).

Numerous degradation experiments of TCE in the presence of zero-valent metals have shown that the process is first order and can be 5 to 15 orders of magnitude greater than natural abiotic rates (e.g., Focht et al., 1996; Gavaskar et al., 1998; Gillham et al., 1997; Gillham and O'Hannesin, 1994; Orth, 1992; Orth and Gillham, 1996). Other batch sorption studies have reported evidence for nonequilibrium sorption (Burris et al., 1995, 1998) that can result in more complex degradation processes and chemical nonequilibrium transport. Casey et al. (2000b) used effluent miscible-displacement experiments to study the fate and transport processes of dissolved concentrations of TCE flowing through water-saturated zero-valent metal filings. They reported breakthrough curves of TCE and its degradation daughter product, ethylene, and described the breakthrough curves by means of equilibrium and nonequilibrium convective–dispersive

F.X.M. Casey, Dep. of Soil Science, North Dakota State Univ., Fargo, ND 58105. J. Šimůnek, George E. Brown Jr. Salinity Lab., USDA-ARS, Riverside, CA 92507. Received 23 Oct. 2000. *Corresponding author (Francis_Casey@NDSU.NoDak.edu).

Published in J. Environ. Qual. 30:1354–1360 (2001).

Abbreviations: L, length; M, mass; T, time; TCE, trichloroethylene.

models. Casey et al. (2000b) did not find other degradation products in their effluent breakthrough curves. Furthermore, in their study they applied the model inversion only to the transport of TCE and then used the optimized transformation coefficients to obtain a reasonable prediction of the ethylene breakthrough curves.

The objective of this study was to modify the equilibrium–nonequilibrium transport model HYDRUS-1D by including an inverse solution that allows simultaneous fit of multiple breakthrough curves resulting from transformation reactions. This modification can improve the interpretation of various transformation reactions, especially when complex transport processes occur. It has been shown previously (e.g., Eching and Hopmans, 1993; Inoue et al., 2000) that simultaneous fit of related information (e.g., pressure heads and outflow during outflow experiments, or pressure heads and concentrations during infiltration experiments) can result in significant reduction of confidence intervals of optimized parameters and thus more reliable determination of governing processes. The HYDRUS-1D model was modified to solve equilibrium and nonequilibrium transport models inversely for multiple solutes subject to sequential transformation reactions. The zero-valent metal miscible-displacement experiments from the Casey et al. (2000b) study were used to demonstrate the inverse application of the modified HYDRUS-1D model. The columns that Casey et al. (2000b) used for the miscible displacement study were packed with iron (Fe) or iron coated in copper (Cu–Fe). It will be shown that the confidence intervals of the optimized parameters improve when information about both TCE and ethylene breakthrough curves is used as opposed to only using information from the TCE breakthrough curve.

MATERIALS AND METHODS

Mathematical Models and Inverse Solution

The following set of coupled differential equations governs the one-dimensional, convective–dispersive, linear-equilibrium transport of a sequence of solutes consecutively undergoing degradation and transformation (van Genuchten, 1985):

$$R_1\frac{\partial C_1}{\partial t} = D\frac{\partial^2 C_1}{\partial x^2} - v\frac{\partial C_1}{\partial x} - \gamma_1\frac{\rho_b K_{d,1}}{\theta}C_1 \qquad [1a]$$

$$R_i\frac{\partial C_i}{\partial t} = D\frac{\partial^2 C_i}{\partial x^2} - v\frac{\partial C_i}{\partial x} - \gamma_i\frac{\rho_b K_{d,i}}{\theta}C_i + \gamma_{i-1}\frac{\rho_b K_{d,i}}{\theta}C_{i-1} \quad (i \geq 2) \qquad [1b]$$

where C_i is the solution concentration (M L^{-3}), D is the hydrodynamic dispersion (L^2 T^{-1}), v is velocity (L T^{-1}), x is distance (L), t is time (T), γ_i is the first-order degradation rate constant (T^{-1}), $K_{d,i}$ is the distribution coefficient (L^3 M^{-1}), ρ_b is the bulk density (M L^{-3}), θ is the volumetric water content (L^3 L^{-3}), and the retardation factor R_i (unitless) is given by:

$$R_i = 1 + \frac{\rho_b K_{d,i}}{\theta} \qquad [2]$$

where the subscript i denotes the i^{th} chain member in the transformation reaction. For the purposes of this study, degradation was considered to be a surface process (Burris et al., 1995). Hence, it was assumed in Eq. [1] that degradation occurs only in the sorbed phase.

Equations [1a,b] and [2] can be extended to include the concept of nonequilibrium two-site adsorption–desorption reactions (Selim et al., 1977; van Genuchten and Wagenet, 1989; Gamerdinger et al., 1990). Sorption on labile exchange sites or Type-1 sites (signified by subscript S1) is assumed to be instantaneous, while on remaining resistant exchange sites or Type-2 sites (signified by subscript S2), sorption is kinetic. The following expressions govern nonequilibrium mass transport for a homogeneous system during steady-state water flow:

$$\left(1 + \frac{\rho_b f K_{d,1}}{\theta}\right)\frac{\partial C_1}{\partial t} = D\frac{\partial^2 C_1}{\partial x^2} - v\frac{\partial C_1}{\partial x} - \frac{\alpha_1\rho_b}{\theta}[(1-f)K_{d,1}C_1 - S_{S2,1}] - \gamma_{S1,1}\frac{f\rho_b K_{d,1}}{\theta}C_1 \qquad [3a]$$

$$\left(1 + \frac{\rho_b f K_{d,i}}{\theta}\right)\frac{\partial C_i}{\partial t} = D\frac{\partial^2 C_i}{\partial x^2} - v\frac{\partial C_i}{\partial x} - \frac{\alpha_i\rho_b}{\theta}[(1-f)K_{d,i}C_i - S_{S2,i}] - \gamma_{S1,i}\frac{f\rho_b K_{d,i}}{\theta}C_i + \gamma_{S1,i-1}\frac{f\rho_b K_{d,i-1}}{\theta}C_{i-1} + \frac{\rho_b}{\theta}\gamma_{S2,i-1}S_{S2,i-1} \quad (i \geq 2) \qquad [3b]$$

where f is the fraction of exchange sites assumed to be at equilibrium (unitless), $\gamma_{S1,i}$ represents solid phase degradation rate constants associated with the equilibrium sorption sites (T^{-1}), $\gamma_{S2,i}$ represents solid phase degradation rate constants associated with the nonequilibrium sorption sites (T^{-1}), and α_i is the first-order kinetic rate sorption constant (T^{-1}). In this study we assumed that the transformation rates were the same on both equilibrium and kinetic sorption sites ($\gamma_{S1,i} = \gamma_{S2,i}$) and that degradation only occurred in the sorbed phase. Mass conservation equations for the nonequilibrium sites ($S_{S2,i}$, M M^{-1} soil) are given by (van Genuchten and Wagenet, 1989):

$$\frac{\partial S_{S2,i}}{\partial t} = \alpha_i[(1-f)K_{d,i}C_i - S_{S2,i}] - \gamma_{S2,i}S_{S2,i} \qquad [4]$$

HYDRUS-1D Version 2.0 (Šimůnek et al., 1998a) numerically solves either the *equilibrium model* (Eq. [1a,b] and [2]) or the *nonequilibrium model* (Eq. [3a,b] and [4]) using Galerkin-type linear finite element schemes. Additionally, HYDRUS-1D may be applied inversely so that the model solution can be fit to the measured data. However, Version 2.0 of HYDRUS-1D could inversely solve the equilibrium or nonequilibrium transport models only for the first solute in the chain of transformation reactions (i.e., C_1 in Eq. [1a] or [3a]). Thus modifications were needed to allow HYDRUS-1D to simultaneously fit breakthrough curves of several solutes undergoing sequential first-order transformation reactions.

Šimůnek et al. (1998a) described the method of parameter optimization used in HYDRUS-1D, where the numerical model solution is fit to measured data. This is done by iteratively changing model parameters and thus improving model fits to the measured data until a desired degree of precision is obtained. The simulated results that are optimized are used together with the measured data to create an objective function, Φ (Šimůnek et al., 1998b):

$$\Phi(\boldsymbol{b},q) = \sum_{k=1}^{m} y_k \sum_{j=1}^{n_k} w_{j,k}\left[q_k^*(x,t_j) - q_k(x,t_j,\boldsymbol{b})\right]^2 \qquad [5]$$

where the right-hand side represents deviations between the measured and calculated space–time variables (e.g., concentrations at different times in the flow domain). In Eq. [5], m

Table 1. Physical properties of 40-mesh zero-valent metal packing material for two columns.

Property	Packing material	
	Iron	Copper-coated iron
Bulk density, g cm^{-3}	2.42	3.09
Particle density, g cm^{-3}	7.10	6.36
Specific surface area, m^2 g^{-1}†	5.76	3.73
Pore volume, mL	29.40	22.90
Surface area concentration, m^2 L^{-1}‡	21 147	
Volumetric water content, cm^3 cm^{-3}	0.66	0.51

†Measured using the BET method (Brunauer et al., 1938).
‡Calculated after Johnson et al. (1996).

is the number of different sets of measurements, n_k is the number of measurements in a particular measurement set, $q_k^*(x,t_j)$ represents specific measurements at time t_j for the k^{th} measurement set at location x, $q_k(x,t_j\boldsymbol{b})$ is the corresponding model prediction for the vector of optimized parameters $\boldsymbol{b}$ (e.g., K_d, D, α, and γ), and y_k and $w_{j,k}$ are weights associated with a particular measurement set or point, respectively. Minimization of Φ is done by the Levenberg–Marquardt nonlinear minimization algorithm (Marquardt, 1963). HYDRUS-1D was modified to include simultaneous parameter optimization for multiple solute breakthrough curves resulting from transformation reactions. To do this, the code was amended to include parameters from the secondary breakthrough curves (i.e., $i > 1$ in Eq. [1b, 2, 3b, and 4]) into the Φ (Eq. [5]). The objective function, which includes parameters from multiple breakthrough curves, can then be minimized using the Levenberg–Marquardt algorithm so that the model solution is fit simultaneously to the measured data of TCE and its degradation daughter products. The breakthrough curves of TCE and its degradation products were considered as different measurement sets. Weights y_k were selected such that contributions of residuals of each breakthrough curve were about equal, while weights $w_{j,k}$ were set equal to one.

HYDRUS-1D also specifies the upper and lower bounds of the 95% confidence level around each fitted parameter $\boldsymbol{b}$. It is desirable that the real value of the target parameter always be located in a narrow interval around the estimated mean as obtained with the optimization program. Large confidence limits indicate that the results are not very sensitive to the value of a particular parameter (Šimůnek et al., 1998a).

To compare optimized γ values with previously reported values, it was important to consider the specific surface area (a_s, L^2 M^{-1}) of the zero-valent metal. Johnson et al. (1996) was able to compare observed degradation rates (γ_{obs}, T^{-1}) from several studies by normalizing the γ_{obs} values according to the surface area of the zero-valent metals. The following relation was presented by Johnson et al. (1996):

$$\gamma_{obs} = \gamma_{norm} a_s \rho_m \quad [6]$$

where γ_{norm} is the normalized degradation rate (L^3 T^{-1} L^{-2}) and ρ_m is the mass concentration of zero-valent metal (M L^{-3} of solution). The terms a_s and ρ_m multiplied together equal the surface area concentration of the zero-valent metal (L^2 L^{-3} of solution; Table 1).

Experimental Procedure

Casey et al. (2000b) described in details the experimental procedures. Two columns (21.4-mm diameter and 124-mm length), packed with 40-mesh iron filings (Fe; Fisher Scientific, Pittsburgh, PA[1]) or 40-mesh Fisher iron filings plated with 1.78% copper (Cu–Fe), were saturated and used for all miscible-displacement experiments. Table 1 shows the physical properties of the packing material for the two columns. Three experiments were run on each column where a pulse of one pore volume of 42 mg L^{-1} TCE was passed through the columns at pore water velocities of 12.4 (denoted as fast), 6.2 (intermediate), or 3.1 (slow) mm min^{-1}. These pore water velocities resulted in one pore volume being displaced every 10, 20, or 40 min, and the order in which the experiments were run was fast, intermediate, and slow. Column effluent was sampled every 5 min for each experiment and diverted to an online high performance liquid chromatography (HPLC) system. The experimental displacement system is described in depth by Casey et al. (2000a). The on-line HPLC was equipped with a Beckman (Fullerton, CA) 128 diode-array flow through photo detector capable of separating out TCE and its daughter products (1,1-dichloroethylene; 1,2-cis-dichloroethylene; 1,2-trans-dichloroethylene; vinyl chloride; and ethylene) and determining their concentrations in the effluent. The detection limit of TCE and its degradation daughter products was approximately 0.01 mg L^{-1}. Casey et al. (2000b) described the analytical procedures in detail.

[1]Names of all products or brands are provided solely for the reader's information and do not imply endorsement of individual brands, nor criticism of similar suitable products.

RESULTS AND DISCUSSION

Figures 1 and 2 present the breakthrough curves of TCE and ethylene from the Casey et al. (2000b) study and the corresponding inverse solutions to the equilibrium and nonequilibrium models from the current study. Trichloroethylene and ethylene were the only products detected in the column effluent. Excellent descriptions of the TCE and ethylene breakthrough curves were obtained when both curves were fitted simultaneously. This is reflected by the relatively high coefficients of determination (r^2; ranging from 0.94 to 1.00 for the equilibrium model and 0.96 to 1.00 for the nonequilibrium model; Table 2). These correlations for the combined fit of the TCE and ethylene breakthrough curves were much better than those reported by Casey et al. (2000b) (r^2 = 0.69 to 0.99 for the equilibrium model, 0.91 to 0.99 for the nonequilibrium model). Casey et al. (2000b) were only able to inversely fit the TCE breakthrough curves and predict, not fit, the ethylene breakthrough curves. Significant improvement in description of the ethylene breakthrough curves in comparison with the Casey et al. (2000b) study was registered, especially for slow water flow rates.

Table 2 presents the optimized parameters from the inverse solutions to the equilibrium and nonequilibrium models that were simultaneously fitted to the TCE and ethylene breakthrough curves. For the equilibrium model, γ_{TCE}, $\gamma_{ethylene}$, $K_{d,TCE}$, and $K_{d,ethylene}$ values were simultaneously optimized to their corresponding breakthrough curves (indicated by the subscripts TCE or ethylene). The source for the ethylene production came directly from the degradation of TCE. Dispersivity ($\lambda = D/v$) values were assumed to be identical for the TCE and ethylene breakthrough curves, and hence estimated from both curves simultaneously. For the nonequilibrium model, γ_{TCE}, $\gamma_{ethylene}$, $K_{d,TCE}$, $K_{d,ethylene}$, α_{TCE}, and $\alpha_{ethylene}$ were simultaneously optimized to their corresponding breakthrough curves. Note that we assume that the transformation rates γ for both TCE and ethylene are

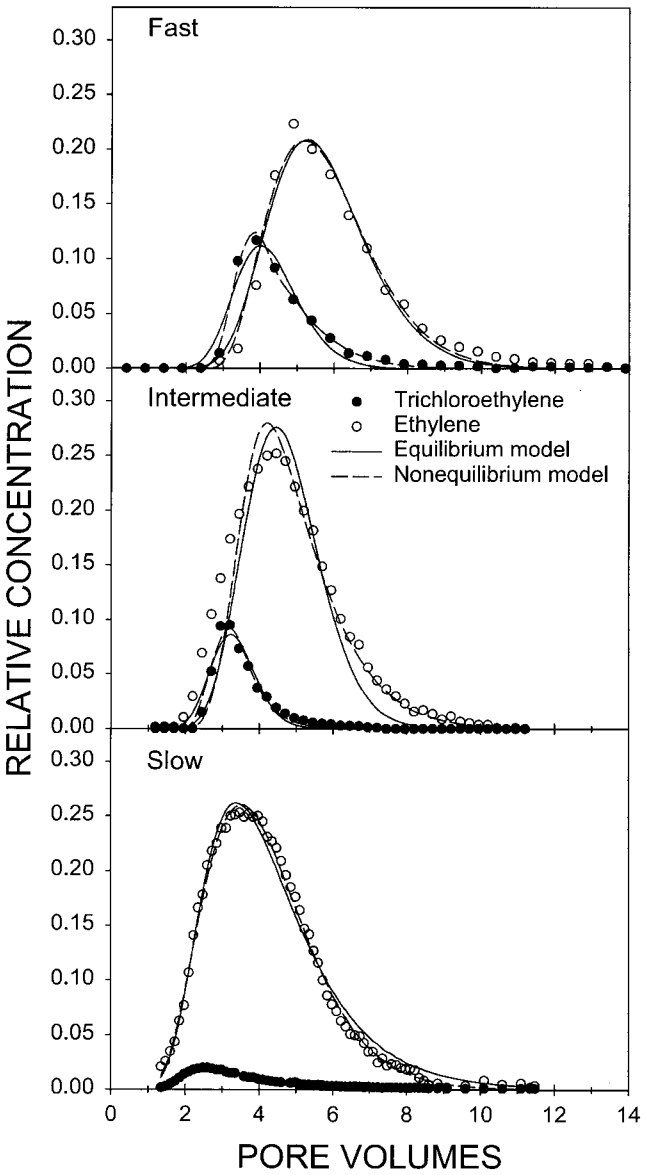

Fig. 1. Breakthrough curves from the column filled with iron filings (Fe column) for the fast, intermediate, and slow flow rates. Inverse model solutions to the equilibrium (Eq. [1a,b and 2]) and nonequilibrium (Eq. [2a,b and 3]) models are also plotted.

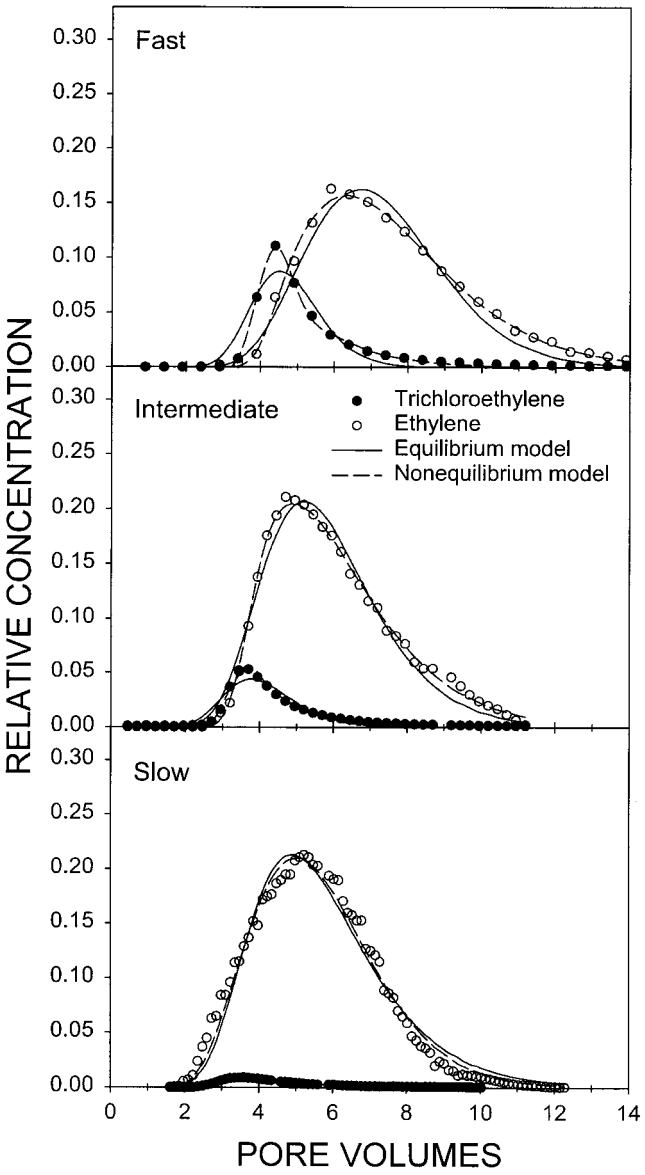

Fig. 2. Breakthrough curves from the column filled with iron fillings coated with copper (Cu–Fe column) for the fast, intermediate, and slow flow rates. Inverse model solutions to the equilibrium (Eq. [1a,b and 2]) and nonequilibrium (Eq. [2a,b and 3]) models are also plotted.

the same on both equilibrium and kinetic sorption sites and only take place in the sorbed phase. We also assumed similar f values for the TCE and ethylene breakthrough curves. Assuming similar λ and f values for the concurrent TCE and ethylene breakthrough curves seems reasonable because both solutes passed through the exact same column filled with the exact same medium (Bear, 1972).

Optimized dispersivities (λ) were about an order of magnitude larger for the equilibrium model than for the nonequilibrium model (Table 2). This is a typical result of fitting breakthrough curves and not taking into account all underlying processes, which may cause the model code to move the effects of the unaccounted processes into another process. In our case, the kinetic sorption was not accounted for in the equilibrium model, which may have moved the kinetic sorption effect into the dispersion term. Values of both γ and K_d parameters for both soil columns are about the same for the equilibrium and nonequilibrium models.

Simultaneous inversion places additional constraint on the inverse solution, which improved the stability and reliability of the parameter estimates by reducing the confidence intervals (Šimůnek et al., 1998b). Casey et al. (2000b) obtained significant cross-correlations between optimized parameters and their correspondingly large confidence intervals when they optimized nonequilibrium model solute transport parameters (λ, f, K_d, γ, and α) to the TCE breakthrough curves only. The 95% confidence intervals of optimized parameters from the Casey et al. (2000b) study often spanned physically nonrealistic values, such as negative values of K_d and

Table 2. Values of the equilibrium (Eq. [1a,b, and 2]) and nonequilibrium (Eq. [3a,b and 4]) transport model parameters† with 95% confidence intervals (in parentheses) for the simultaneous inverse fit of the trichloroethylene (TCE) and ethylene breakthrough curves.‡

Experiment	Parameter								
	λ	f	$K_{d,TCE}$	γ_{TCE}	α_{TCE}	$K_{d,ethylene}$	$\gamma_{ethylene}$	$\alpha_{ethylene}$	r^2
	cm		L kg^{-1}	min^{-1}		L kg^{-1}	min^{-1}		
	Equilibrium transport model								
Iron column									
Fast	0.34 (0.05)		0.62 (0.01)	0.048 (0.002)		1.08 (0.06)	0.004 (0.004)		0.95
Intermediate	0.24 (0.05)		0.46 (0.02)	0.051 (0.001)		0.85 (0.04)	0.004 (0.002)		0.94
Slow	1.58 (0.15)		2.06 (0.14)	0.052 (0.001)		1.57 (0.04)	0.001 (0.000)		0.99
Copper-coated iron column									
Fast	0.31 (0.06)		0.62 (0.02)	0.046 (0.048)		1.18 (0.04)	0.002 (0.001)		0.97
Intermediate	0.54 (0.07)		0.59 (0.03)	0.037 (0.002)		0.85 (0.02)	0.002 (0.001)		0.96
Slow	0.82 (0.07)		0.82 (0.07)	0.026 (0.002)		0.78 (0.02)	0.001 (0.000)		1
	Nonequilibrium transport model								
Iron column									
Fast	0.02 (0.01)	0.55 (0.02)	0.80 (0.03)	0.042 (0.002)	0.145 (0.029)	1.05 (0.04)	0.003 (0.003)	0.272 (0.079)	0.96
Intermediate	0.04 (0.01)	0.64 (0.05)	0.52 (0.07)	0.048 (0.007)	0.118 (0.109)	0.90 (0.07)	0.002 (0.005)	0.090 (0.046)	0.98
Slow	0.18 (0.18)	0.21 (0.04)	2.86 (0.39)	0.019 (0.001)	0.021 (0.004)	1.23 (0.05)	0.001 (0.001)	0.080 (0.019)	0.98
Copper-coated iron column									
Fast	0.03 (0.00)	0.58 (0.02)	0.83 (0.03)	0.037 (0.001)	0.071 (0.008)	1.16 (0.02)	0.001 (0.003)	0.139 (0.058)	0.98
Intermediate	0.02 (0.02)	0.51 (0.03)	0.65 (0.04)	0.037 (0.001)	0.066 (0.015)	0.89 (0.02)	0.001 (0.001)	0.070 (0.006)	1
Slow	0.05 (0.07)	0.18 (0.15)	1.17 (0.67)	0.022 (0.007)	0.028 (0.026)	0.70 (0.08)	0.001 (0.011)	0.065 (0.019)	0.99

† λ, dispersivity (=hydrodynamic dispersion/velocity); K_d, distribution coefficient; f, fraction of Type-1 sorption sites; α, first-order mass transfer constant; γ, reaction rate constant; r^2, coefficient of determination.
‡ Subscripts "TCE" and "ethylene" signify parameters for the respective breakthrough curve.

f. Fitted TCE breakthrough curves obviously did not contain enough information to allow simultaneous fitting of five parameters of the nonequilibrium transport model. This was the case especially for the slow flow rate experiments, when most TCE was already transformed before reaching the end of the soil column and fitting was applied to the breakthrough curves with relatively small concentrations (less than one hundredth of the initially applied concentration). As a result, optimized parameters were hardly identifiable, confidence in them was relatively low, and also the predictions of the ethylene breakthrough curves were not very good. This problem was overcome when both TCE and ethylene breakthrough curves were fitted simultaneously. Confidence intervals of all optimized parameters, as well as their cross-correlations, were reduced dramatically for both equilibrium and nonequilibrium models.

The nonequilibrium model described the TCE and ethylene breakthrough curves significantly better for the fast flow rates for both Fe and Cu–Fe columns than the equilibrium model. However, as the flow rate decreased, differences between the equilibrium and nonequlibrium model fits decreased until they were nearly identical for the slow flow rate. This trend was more prevalent when the inverse model solution was applied to both TCE and ethylene, and not just to TCE, as was done by Casey et al. (2000b). This trend also suggested that some type of mass transfer limitation existed at the faster flow rates, such as diffusion to the iron surface (Burt, 1999), a process that exhibits itself as a kinetically controlled sorption. Burris et al. (1998) suggested that a rate-limiting step may be present in the transformation of TCE as it desorbs from reactive sites on zero-valent metal. Although the simultaneous inverse fit to the TCE and ethylene breakthrough curves can provide more insight into which models best describe the data, more experiments need to be performed to verify this assertion.

The more complex nonequilibrium transport model has more parameters, which should improve the fit of the model to the data. However, good model fits do not necessarily mean more accurate identification of the underlying transport processes because the model solutions may not be unique, resulting in unrealistic parameter estimates or large confidence intervals. Therefore, complex transport models need to be used with discretion, by using as many as possible independent estimates of unknown transport parameters.

To verify the results found from this study, some of the model parameters were compared with independently estimated values from previous batch and degradation experiments. Numerous zero-valent metal degradation experiment studies exist where first-order degradation rates for TCE have been reported. For example, Tratnyek et al. (1997) summarized a collection of degradation rates (Fig. 3) that were normalized according to surface area (Johnson et al., 1996). The normalized TCE degradation rates from this study fell within the range of previously reported values (Fig. 3), but they were at the low end of the range. Burt (1999) used batch and column experiments to study the degradation of another chlorinated aliphatic hydrocarbon, perchloroethylene, in the presence of zeolites impregnated with zero-valent metals. He found that the degradation rate values estimated from the column experiments were lower than values estimated from batch experiments and suggested that the difference was caused by physical mass transfer limitations. This may suggest why the degradation rate values from this study fell at the lower end of the range reported by previous researchers. Furthermore, a linearized K_d value (1.47 L kg^{-1}) from Burris et al. (1995)

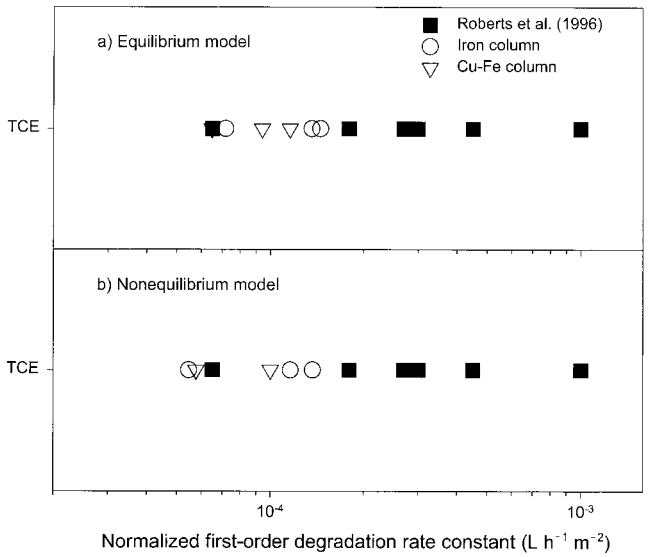

Fig. 3. A comparison of normalized degradation rates from this study to previous studies. The normalized degradation rates were obtained from curve fits using the (*a*) equilibrium and (*b*) nonequilibrium sorption models. Figure adapted from Tratnyek et al. (1997) and is reprinted by permission of Ground Water Monitoring & Remediation (Copyright 1997).

was calculated and found to be within the range of K_d values obtained in this study (Table 2).

CONCLUSION

The HYDRUS-1D model was successfully modified to include inverse solutions for solutes undergoing transport and transformation. The inverse technique was applied to sample TCE and ethylene breakthrough curves and provided more stabile and accurate estimates of the transport parameters. The improvement lead to more reliable identification of underlying transport processes, which was indicated by excellent correlation between the model predictions and measured data, notwithstanding added constraints to the inverse solution. Confidence intervals of optimized parameters, obtained by analyzing TCE and ethylene breakthrough curves simultaneously, were significantly reduced compared with those obtained using only the TCE breakthrough curve. The parameters that were estimated using the modified HYDRUS-1D model were consistent with independently obtained parameters from previous studies. The inverse application presented in this study should lend better understanding of subsurface transport processes involving solutes that undergo transformation reactions.

REFERENCES

Appleton, E.L. 1996. A nickel–iron wall against contaminated groundwater. Environ Sci. Technol. 30:536A–539A.

Bear, J. 1972. Dynamics of fluids in porous media. Dover Publ., New York.

Brunauer, S., P.H. Emmett, and E. Teller. 1938. Adsorption of gases in multimolecular layers. J. Am. Chem. Soc. 60:309–319.

Burris, D.R., M.A. Allen-King, V.S. Manoranjon, T.J. Campbell, G.A. Loraine, and B. Deng. 1998. Chlorinated ethene reduction by cast iron: Sorption and mass transfer. J. Environ. Eng. 124:1012–1019.

Burris, D.R., T.J. Campbell, and V.S. Manoranjon. 1995. Sorption of trichloroethylene and tetrachloroethylene in a batch reactive metallic iron–water system. Environ. Sci. Technol. 29:2850–2855.

Burt, T.A. 1999. Percholoroethylene and chromate sorption/reduction using a surfactant-modified zeolite/zero valent iron pellet. M.S. thesis. New Mexico Inst. of Mining Technol., Socorro, NM.

Casey, F.X.M., R.P. Ewing, and R. Horton. 2000a. Automated system for miscible-displacement through soil of multiple volatile organic compounds. Soil Sci. 165:841–847.

Casey, F.X.M., S.K. Ong, and R. Horton. 2000b. Degradation and transformation of trichloroethylene in miscible-displacement experiments through zero-valent metals. Environ. Sci. Technol. 34:5023–5029.

Castro, C.L., and D.E. Rolston. 1977. Organic phosphate transport and hydrolysis in soil: Theoretical and experimental evaluation. Soil. Sci. Soc. Am. J. 41:1085–1092.

Eching, S.O., and J.W. Hopmans. 1993. Optimization of hydraulic functions from transient outflow and soil water pressure data. Soil Sci. Soc. Am. J. 57:1167–1175.

Evans, C.V., L.S. Morton, and G. Harbottle. 1997. Pedologic assessment of radionuclide distributions: Use of a radio-pedogenic index. Soil Sci. Soc. Am. J. 61:1440–1449.

Focht, R.M., J.L. Vogan, and S.F. O'Hannesin. 1996. Field application of reactive iron walls for in-situ degradation of volatile organic compounds in groundwater. Remediation 6:81–94.

Gamerdinger, A.P., R.J. Wagenet, and M.Th. van Genuchten. 1990. Application of two-site/two-region models for studying simultaneous nonequilibrium transport and degradation of pesticides. Soil Sci. Soc. Am. J. 54:957–963.

Gavaskar, A., B.M. Sass, E. Drescher, L. Cumming, D. Giammar, and N. Gupta. 1998. Enhancing the reactivity of permeable barrier media. p. 1:91–96. *In* G.B.Wickramanayake and R.E. Hinchee (ed.) Designing and applying treatment technologies. Proc. of the 1st Int. Conf. on Remediation of Chlorinated and Recalcitrant Compounds, Monterey, CA. 18–21 May 1998. Battelle Press, Columbus, OH.

Gillham, R.W., and S.F. O'Hannesin. 1994. Enhanced degradation of halogenated aliphatics by zero-valent iron. Ground Water 32:958–967.

Gillham, R.W., S.F. O'Hannesin, M.S. Odziemkowski, R.A. Garcia-Delgado, R.M. Focht, W.H. Matulewicz, and J.E. Rhodes. 1997. Enhanced degradation of VOCs: Laboratory and pilot-scale field demonstration. p. 858–863. *In* 2nd Int. Containment Technol. Conf., St. Petersburg, FL. 9–12 Feb. 1997. U.S. Dep. of Energy, Washington, DC.

Inoue, M., J. Šimůnek, S. Shiozawa, and J.W. Hopmans. 2000. Estimation of soil hydraulic and solute transport parameters from transient infiltration experiments. Adv. Water Resour. 23:677–688.

Johnson, T.L., M.M. Scherer, and P.G. Tratnyek. 1996. Kinetics of halogenated organic compound degradation by iron metal. Environ. Sci. Technol. 30:2634–2640.

Kool, J.B., J.C. Parker, and M.Th. Van Genuchten. 1985. Determining soil hydraulic properties from one-step outflow experiments by parameter estimation: I. Theory and numerical studies. Soil Sci. Soc. Am. J. 49:1348–1354.

Marquardt, D.W. 1963. An algorithm for least-squares estimation of nonlinear parameters. J. Soc. Ind. Appl. Math. 11:431–441.

Mishra, B.K., and C. Misra. 1991. Kinetics of nitrification and nitrate reduction during leaching of ammonium nitrate through a limed Ultisol profile. J. Indian Soc. Soil Sci. 39:221–228.

Misra, C., D.R. Nielsen, and J.W. Biggar. 1974. Nitrogen transformation in soil during leaching: II. Steady state nitrification and nitrate reduction. Soil Sci. Soc. Am. Proc. 38:294–299.

National Academy of Science. 1994. Alternatives for ground water cleanup. Report of the National Academy of Science Committee of Ground Water Cleanup Alternatives. National Academy Press, Washington, DC.

Orth, S.W. 1992. Mass balance of the degradation of trichloroethylene in the presence of iron filings. M.S. thesis. Univ. of Waterloo, ON, Canada.

Orth, S.W., and R.W. Gillham. 1996. Dechlorination of trichlorethene in aqueous solution using Fe(0). Environ. Sci. Technol. 30:66–71.

Schaerlaekens, J., D. Mallants, J. Šimůnek, M.Th. van Genuchten, and J. Feyen. 1999. Numerical simulation of transport and sequential biodegradation of chlorinated aliphatic hydrocarbons using CHAIN_2D. Hydrol. Processes 13:2847–2859.

Selim, H.M., J.M. Davidson, and P.S.C. Rao. 1977. Transport of reactive solutes through multilayered soils. Soil Sci. Soc. Am. J. 41:3–10.

Šimůnek, J., M. Šejna, and M.Th. van Genuchten. 1998a. The HY-

DRUS-1D software package for simulating the one-dimensional movement of water, heat, and multiple solutes in variably-saturated media. Version 2.0, IGWMC-TPS-70. Int. Ground Water Modeling Center, Colorado School of Mines, Golden, CO.
Šimůnek, J., O. Wendroth, and M.Th. van Genuchten. 1998b. Parameter estimation analysis of the evaporation method for determining soil hydraulic properties. Soil Sci. Soc. Am. J. 62:894–905.
Tratnyek, P.G., T.L. Johnson, M.M. Scherer, and G.R. Eykholt. 1997. Remediating ground water with zero-valent metals: Chemical considerations in barrier design. Ground Water Monit. Rem. 17:108–114.
van Genuchten, M.Th. 1981. Non-equilibrium transport parameters from miscible displacement experiments. Res. Rep. 119. U.S. Salinity Lab., Riverside, CA.
van Genuchten, M.Th. 1985. Convective–dispersive transport of solutes involved in sequential first-order decay reactions. Comp. Geosci. 11:129–147.
van Genuchten, M.Th., and R.J. Wagenet. 1989. Two-site/two-region models for pesticide transport and degradation: Theoretical development and analytical solutions. Soil. Sci. Soc. Am. J. 53:1303–1310.
Viswanathan, H.S., B.A. Robinson, A.J. Valocchi, and I.R. Triay. 1998. A reactive transport model of neptunium migration from the potential repository at Yucca Mountain. J. Hydrol. 209:251–280.

Seasonal Leaching and Biodegradation of Dicamba in Turfgrass

J. W. Roy, J. C. Hall, G. W. Parkin,* C. Wagner-Riddle, and B. S. Clegg

ABSTRACT

The leaching of surface-applied herbicides, such as dicamba (2-methoxy-3,6-dichlorobenzoic acid), to ground water is an environmental concern. Seasonal changes in soil temperature and water content, affecting infiltration and biodegradation, may control leaching. The objectives of this study were to (i) investigate the leaching of dicamba applied to turfgrass, (ii) measure the degradation rate of dicamba in soil and thatch in the laboratory under simulated field conditions, and (iii) test the ability of the model EXPRES (containing LEACHM) to simulate the field transport and degradation processes. Four field lysimeters, packed with sandy loam soil and topped with Kentucky bluegrass (*Poa pratensis* L.) sod, were monitored after receiving three applications (May, September, November) of dicamba. Concentrations of dicamba greater than 1 mg L^{-1} were detected in soil water. Although drying of the soil during the summer prevented deep transport, greater leaching occurred in late autumn due to increased infiltration. From the batch experiment, the degradation rate for dicamba in thatch was 5.9 to 8.4 times greater than for soil, with a calculated half-life as low as 5.5 d. Computer modeling indicated that the soil and climatic conditions would influence the effectiveness of greater degradation in thatch for reducing dicamba leaching. In general, EXPRES predictions were similar to observed concentration profiles, though peak dicamba concentrations at the 10-cm depth tended to be higher than predicted in May and November. Differences between predictions and observations are probably a result of minor inaccuracies in the water-flow simulation and the model's inability to modify degradation rates with changing climatic conditions.

Leaching of pesticides through the soil to the ground water is a concern since these chemicals may affect the quality of drinking water supplies and surface water ecosystems. Dicamba, a postemergent herbicide commonly used to control broadleaf weeds in turfgrass, has been detected in ground water (Koterba et al., 1993; Cox, 1994). The acceptable limit for dicamba in drinking water is 200 μg L^{-1} in the United States and 120 μg L^{-1} in Canada (Caux et al., 1993). Based on numerous studies in Canada, Caux et al. (1993) calculated that 8% of the surface water and 2% of the ground water samples contained detectable amounts of dicamba. Cohen et al. (1990) tested the ground water under various golf courses on Cape Cod, MA, and detected dicamba in 1 of the 16 monitoring wells.

Most researchers have found only very low levels of dicamba in infiltrating water and low total mass of leached dicamba when applied to turf. For lawn or golf green conditions, few of the percolate samples collected between 0.10 to 0.20 m below surface had concentrations exceeding 10 μg L^{-1} (Gold et al., 1988; Smith and Bridges, 1996; Snyder and Cisar, 1997). In these previous studies applications took place from spring to late fall, with rates ranging from 0.11 to 0.28 kg ha^{-1}. Although soil cores taken by Snyder and Cisar showed noticeable peaks of dicamba concentration in soil and thatch shortly after application, these rapidly declined over the following 2 wk.

In a field study by Harrison et al. (1993), relatively high concentrations of dicamba were measured in runoff and/or percolate on sloped turf grown on clay topsoil. They applied dicamba at 0.28 kg ha^{-1} in July, August, September, October, and November over 2 yr. The peaks in concentration for leachate samples collected at the 0.15-m depth coincided with the first major irrigation or rainfall within a week after application, although Harrison et al. (1993) considered the irrigation events extreme. The mean concentrations (three replicate samples) of dicamba in leachate following these events were 11, 21, 22, 118, and 57 μg L^{-1}.

Only recently have researchers modeled the transport of solutes applied to turfgrass. The GLEAMS model greatly overpredicted pesticide leaching below turf (Smith et al., 1993). A number of researchers (Pennell et al., 1990; Costa et al., 1994; Brown et al., 1996) indicated that LEACHM (Wagenet and Hutson, 1987) simulates solute transport in unsaturated soil as well or better than other models. However, LEACHM predicted significantly higher dicamba concentrations in leachate and longer travel times for dicamba transport

J.W. Roy, G.W. Parkin, and C. Wagner-Riddle, Dep. of Land Resource Science, and J.C. Hall and B.S. Clegg, Dep. of Environmental Biology, Univ. of Guelph, Guelph, ON, Canada N1G 2W1. J.W. Roy, current address: Dep. of Earth Sciences, Univ. of Waterloo, Waterloo, ON, Canada N2L 3G1. Received 26 May 2000. *Corresponding author (gparkin@lrs.uoguelph.ca).

Published in J. Environ. Qual. 30:1360–1370 (2001).

Abbreviations: GC–MS, gas chromatography–mass spectrometry; HPLC, high pressure liquid chromatography.